Age of gray matters: Neuroprediction of recidivism

Kent A. Kiehl[a,b,c,d,*], Nathaniel E. Anderson[a], Eyal Aharoni[e], J.Michael Maurer[a,b], Keith A. Harenski[a], Vikram Rao[a], Eric D. Claus[a], Carla Harenski[a], Mike Koenigs[f], Jean Decety[g], David Kosson[h], Tor D. Wager[i], Vince D. Calhoun[a,c,j,k], Vaughn R. Steele[a]

[a] The nonprofit Mind Research Network (MRN) & Lovelace Biomedical, Albuquerque, NM, USA
[b] Department of Psychology, University of New Mexico, Albuquerque, NM, USA
[c] Department of Neurosciences, University of New Mexico, Albuquerque, NM, USA
[d] University of New Mexico School of Law, Albuquerque, NM, USA
[e] Department of Psychology, Georgia State University, Atlanta, GA, USA
[f] Department of Psychiatry, University of Wisconsin-Madison, Madison, WI, USA
[g] Department of Psychology, Department of Psychiatry and Behavioral Neuroscience, University of Chicago, Chicago, IL, USA
[h] Department of Psychology, Rosalind Franklin University, Chicago, IL, USA
[i] Department of Psychology, University of Colorado-Boulder, Boulder, CO, USA
[j] Department of Electrical and Computer Engineering, University of New Mexico, Albuquerque, NM, USA
[k] Department of Psychiatry, University of New Mexico, Albuquerque, NM, USA

ARTICLE INFO

ABSTRACT

Age is one of the best predictors of antisocial behavior. Risk models of recidivism often combine chronological age with demographic, social and psychological features to aid in judicial decision-making. Here we use independent component analyses (ICA) and machine learning techniques to demonstrate the utility of using brain-based measures of cerebral aging to predict recidivism. First, we developed a brain-age model that predicts chronological age based on structural MRI data from incarcerated males ($n = 1332$). We then test the model's ability to predict recidivism in a new sample of offenders with longitudinal outcome data ($n = 93$). Consistent with hypotheses, inclusion of brain-age measures of the inferior frontal cortex and anterior-medial temporal lobes (i.e., amygdala) improved prediction models when compared with models using chronological age; and models that combined psychological, behavioral, and neuroimaging measures provided the most robust prediction of recidivism. These results verify the utility of brain measures in predicting future behavior, and suggest that brain-based data may more precisely account for important variation when compared with traditional proxy measures such as chronological age. This work also identifies new brain systems that contribute to recidivism which has clinical implications for treatment development.

1. Introduction

A practical approach for differentiating risk levels among offenders is to develop algorithms that identify variables that predict how likely inmates are to commit another crime after their release from prison. Meta-analyses have identified several key risk variables including criminogenic needs, demographics, social achievement, socio-economic status, and intelligence (Gendreau et al., 1996). Additional research has identified empirically derived static (e.g., past criminal history, offense type) and dynamic (e.g., impulsivity, drug use, social support) risk factors that have led to significant improvements in predicting future antisocial behavior (Douglas et al., 2002; Harris et al., 1993; Yang et al., 2010). These risk assessment procedures are useful in judicial decision-making and in creating release plans that minimize risk factors (e.g., substance abuse) and accentuate protective factors (e.g., social support, stable employment).

Developments in bio-psycho-social models have identified risk variables with strong relevance to antisocial behavior. Age, for example, is a powerful variable in the prediction the likelihood for antisocial behavior (Gendreau et al., 1996). Indeed, if we consider the release of two inmates from prison, a 25-year-old and a 35-year-old, all else being equal, the 25-year-old is roughly 25% more likely to be re-incarcerated within five years following their release than is the 35-year old (Durose et al., 2014). Age also features prominently in societal decisions about holding people accountable for their behavior, as our treatment of juvenile offenders is categorically different than that of adults.

Chronological age, however, may be an imprecise measure in these risk equations. That is, within the spectrum of all 25-year olds, some of the cohort may be lower than average risk and some may be higher than average risk to re-offend. In other words, chronological age does not account for individual differences in the physiological and neurocognitive aging processes. Recent developments have shown that biological aging of the brain can be quantified using MRI techniques. Franke and colleagues were among the first to develop regression models predicting chronological age from structural MRI of the brain with high accuracy in healthy adults (Franke et al., 2010), as well as children and adolescents (Franke et al., 2012). MRI-based measures of brain-age have subsequently been applied successfully as an indicator of cognitive decline in aging populations (Gaser et al., 2013), and further predicts physiological indices of aging and mortality (Cole, 2017; Cole et al., 2017). Still others have shown relevant effects of brain-age in the context of psychopathology (Koutsouleris et al., 2013; Schnack et al., 2016) and brain injury (Cole et al., 2015). The recognized utility of brain-based measures of aging has expanded into multimodal imaging applications (Brown et al., 2012; Dosenbach et al., 2010), and methods improving the accuracy of these measures continue to progress in these domains.

Despite age being a strong indicator of the likelihood for recidivism, there have been no published attempts applying an MRI-based model of brain-age to the prediction of antisocial behavior. In prior work, our team has demonstrated the utility of brain-based measures of behavioral inhibition in predicting likelihood for rearrest (Aharoni et al., 2013; Steele et al., 2015). Here, we extend this work by developing a brain-based model of age using multivariate analyses of structural MRI data and apply this method to improve prediction of antisocial outcomes. Specifically, we test whether our brain-age measures improve the accuracy of prediction models for rearrest over and above chronological age and other variables used in our prior analyses (Aharoni et al., 2013). To our knowledge, this is the first attempt to develop a brain maturation model to distinguish individuals who are more or less likely to re-offend following release from prison.

2. Materials and methods

All study procedures described below were carried out in accordance with The Code of Ethics of the World Medical Association (Declaration of Helsinki) for experiments involving humans and approved by the Ethical and Independent Review Services. Individuals 18 years of age or older provided written informed consent and individuals younger than 18 years of age provided written informed assent in conjunction with parent/guardian written informed consent.

2.1. Participants

Participants included 1332 male offenders (sample 1) ranging from 12 to 65 years of age ($M = 30.5$, $SD = 11.46$) and 93 male offenders (sample 2 (Aharoni et al., 2013)), ranging from 20 to 52 years of age ($M = 32.94$, $SD = 7.83$) for which follow-up recidivism data was available from official arrest records. None of the participants in sample 1 were included in sample 2. Based on the NIH racial and ethnic classification, 4% of the sample self-identified as American Indian/Alaskan Native, 12% as Black/African American, 1% as Native Hawaiian or other Pacific Islander, 29% as White, 22% as Hispanic/Latino, 1% identified as more than one race, and 30% chose not to respond.

Full-scale IQ was estimated using the Vocabulary and Matrix Reasoning sub-tests of the Wechsler Intelligence Scale for Children – 4th Edition (WISC-IV; Wechsler, 2003) for participants younger than 18 years of age, and the Wechsler Adult Intelligence Scale – 3rd Edition (WAIS-III; (Wechsler, 1997)) for participants older than 18 years of age ($M = 97.13$, $SD = 13.97$)). Mental illness and substance use was assessed using the Kiddie Schedule for Affective Disorders and Schizophrenia (K-SADS; (Kaufman et al., 1997)) for participants younger than

18 years of age and the Structured Clinical Interview for DSM-IV Axis I Disorders – Patient Version (SCID I-P; (First et al., 1997)).

Participants were excluded from analyses for a history of personal or familial bipolar or psychotic disorders, or if they had a full-scale IQ < 70, or were unable to complete a 'research consent test' examining their understanding of the research study. Reported head injuries/concussions were evaluated for each participant: loss of consciousness > 10 mins with persistent symptoms and/or cognitive impairment, or abnormal radiological findings indicating prior head injury were grounds for exclusion. This resulted in the exclusion of approximately 10% of consented volunteers.

2.2. MRI acquisition

T1-weighted MRI scans were acquired on the Mind Research Network (MRN) Siemens 1.5 T Avanto mobile scanner stationed at the prisons using a multi-echo MPRAGE pulse sequence (repetition time = 2530 ms, echo times = 1.64 ms, 3.50 ms, 5.36 ms, 7.22 ms, inversion time = 1100 ms, flip angle = 7°, slice thickness = 1.3 mm, matrix size = 256 × 256) yielding 128 sagittal slices with a resolution of 1.0 mm × 1.0 mm × 1.0 mm. Images were spatially normalized to the Montreal Neurological Institute (MNI) template using SPM12, segmented into gray matter, white matter, and cerebrospinal fluid. Both gray matter volume and density were extracted for analyses. A Jacobian modulation was performed to preserve total volume (Ashburner and Friston, 2000, 2005). Gray matter images were resampled to 2 × 2 × 2 mm and smoothed with a 10 mm full-width at half-maximum (FWHM) Gaussian kernel.

2.3. Experiment 1

ICA of structural MRI (i.e., SBM) was computed from sample 1 (Calhoun et al., 2001; Caprihan et al., 2011; Xu et al., 2009). Thirty volume and density components were extracted using the GIFT toolbox (http://mialab.mrn.org/software/gift). Loading coefficients were extracted for each IC and for each participant. These coefficients were then used in a stepwise linear regression as independent variables (IVs) with chronological age as the dependent variable (DV). We identified 19 brain volume and 19 density components (Figs. 1 & 2; Table 2) accounting for 68.2% and 71.0%, respectively, of the variance in chronological age.

2.4. Experiment 2

Experiment 2 was designed to use the ICs that accounted for chronological age from Experiment 1 to predict future rearrest in an independent set of participants (sample 2). Machine learning techniques were used to identify brain ICs that predicted recidivism from both brain volume and density. Cox proportional hazards regression models using chronological and neural age measures were computed and compared.

Sample 2 participants were followed after release from prison and tracked using official arrest records from 2007 to 2010. The average follow-up period was 21.96 months (range: 1.51 to 49.55 months; see (Aharoni et al., 2013)). Psychopathic traits were assessed among sample 2 participants using the Hare Psychopathy Checklist-Revised (PCL-R; (Hare, 2003)) (M Total Score = 23.41, $SD = 6.89$; scores for $n = 11$ unavailable). Full-scale IQ was estimated using the Vocabulary and Matrix Reasoning sub-tests of the WAIS-III ($M = 94.27$, $SD = 12.75$; n = 11 subjects did not complete IQ). Mental illness and substance dependence was assessed using the SCID I-P (First et al., 1997). An average drug abuse/dependence measure was calculated from the following drug classes: sedatives (6% met for dependence), cannabis (61% met for dependence), stimulants (49% met for dependence), opioids (23% met for dependence), cocaine (56% met for dependence), and hallucinogens (9% met for dependence); substance use scores were unavailable for $n = 13$ participants. Additionally, 54% met
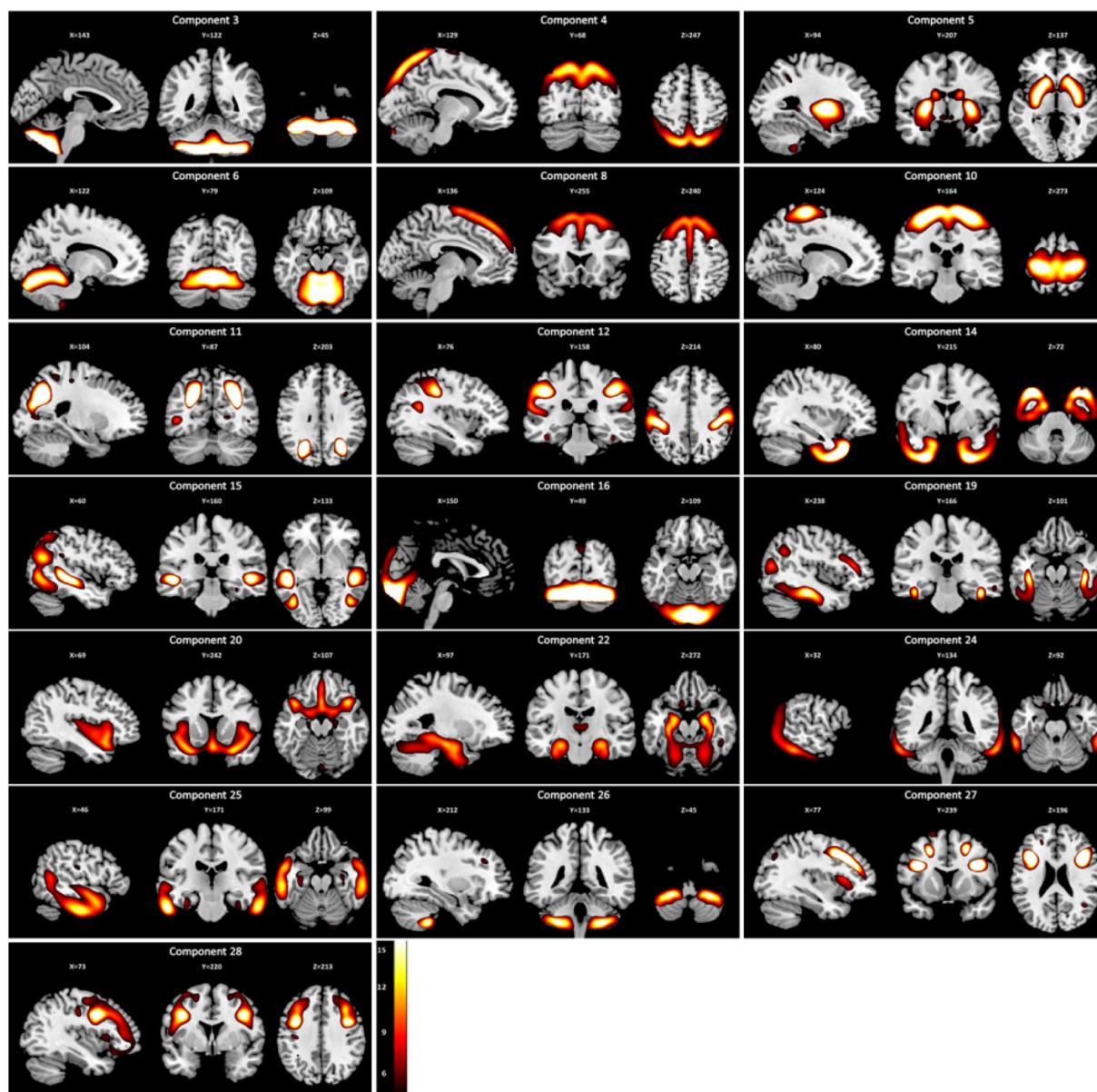
Fig. 1. Source-based morphometry (SBM) of 19 components of gray matter volume identified to account for 68.2% of the variance of chronological age. Components 14 (temporal pole) and 24 (inferior temporal gyrus) were feature selected to be beneficial in predicting rearrest. Components 3 (cerebellum), 4 (inferior and superior parietal gyrus and occipital lobe), 5 (putamen), 6 (cerebellum), 8 (superior and middle frontal gyrus and supplementary motor area), 10 (precentral and postcentral gyrus), 11 (superior parietal gyrus and occipital lobe), 12 (inferior parietal and postcentral gyrus), 14 (temporal pole), 15 (middle temporal gyrus), 16 (cerebellum and lingual gyrus), 19 (fusiform and inferior temporal gyrus), 20 (orbitofrontal cortex and insula), 22 (cerebellum, hippocampus, and amygdala), 25 (middle and inferior temporal gyrus), 26 (cerebellum), 27 (inferior and middle frontal gyrus), and 28 (precentral gyrus) were not selected to be beneficial in predicting rearrest.

criteria for alcohol dependence. Based on the NIH racial and ethnic classification, 5% of the sample self-identified as American Indian/ Alaskan Native, 6% as Black/African American, 22% as White, 41% as Hispanic/Latino, 1% identified as more than one race, and 25% chose not to respond.

2.4.1. Analysis for experiment 2

Using the neural age measures identified in Experiment 1, loading parameters for the ICs were estimated from participants in Experiment 2 using spatio-temporal (dual) regression (Erhardt et al., 2011). In this way, the data in Experiment 2 was projected from the initial ICA calculated on participants from Experiment 1. This step avoids bias in IC definition as none of the participants in Experiment 2 were used to define the ICs related to age. The 19 brain volume measures accounted for 59.0% of variance in age in Experiment 2, compared to 68.2% in

Experiment 1. The 19 density measures accounted for 67.1% of variance in age in Experiment 2 compared to 71.0% in Experiment 1. When combined into a single regression the 19 volume and 19 density variables account for 75.0% of variance in age in Experiment 2.

In an attempt to reduce model complexity in predicting recidivism, we used a sequential K best feature selection with two nested cross validation loops (10-fold for outer loop and 3-fold for inner loop) using Support Vector Machines (SVM) as a criterion function to identify which components were most useful in predicting rearrest (Jain et al., 2000). The 10-fold cross validation outer loop cycles across subjects and the 3-fold inner loop cycles across a set of parameters for the SVM model. The goal of feature selection is to prune the set of IC (or behavioral) variables to identify the best discriminative set. Non-informative features add noise and dimensionality to the data that result in poor classification performance. Sequential K best feature selection selects a set of variables from the input feature set for
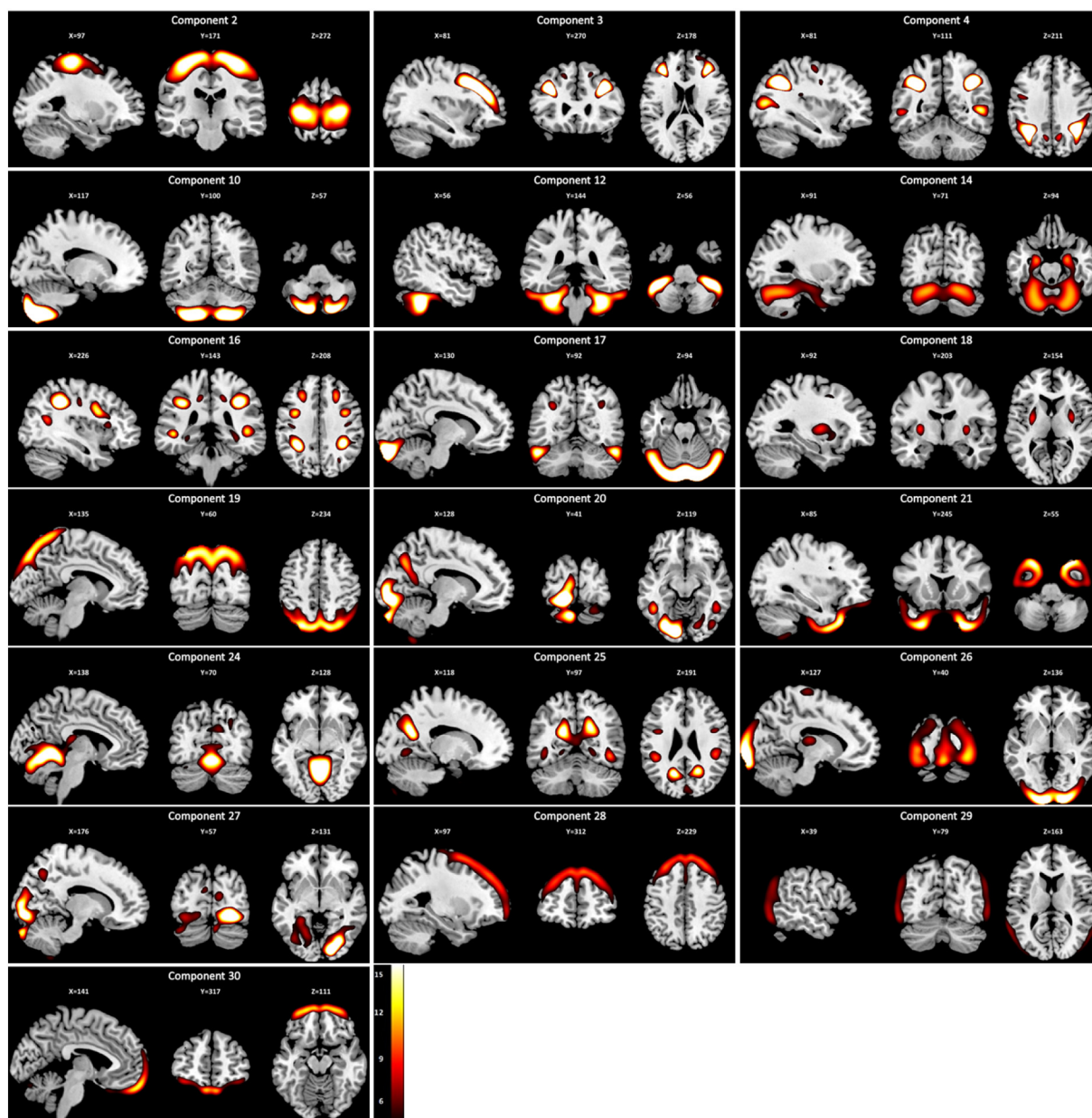
Fig. 2. Source-based morphometry (SBM) of 19 components of gray matter density identified to account for 71.0% of the variance of chronological age. Components 4 (angular gyrus), 16 (inferior parietal gyrus), 21 (temporal pole), 24 (cerebellum), and 26 (occipital lobe) were feature selected to be beneficial in predicting rearrest. Components 2 (precentral and postcentral gyrus), 3 (middle frontal gyrus), 10 (cerebellum), 12 (cerebellum), 14 (cerebellum, hippocampus, and amygdala), 17 (cerebellum), 18 (putamen), 19 (superior parietal gyrus and precuneus), 20 (fusiform gyrus, calcarine fissure, lingual gyrus, and occipital lobe), 25 (precuneus and calcarine fissure), 27 (fusiform gyrus, calcarine fissure, lingual gyrus, and occipital lobe), 28 (superior and middle frontal gyrus), 29 (middle and inferior temporal gyrus), and 30 (orbitofrontal cortex) were not selected to be beneficial in predicting rearrest.

classifying individuals into groups (i.e., rearrested [$n = 50$] versus non-rearrested [$n = 43$]). This feature selection is a method that iterates selecting K best features based on ANOVA F-scores between the two classes of interest. After this step, the scores are averaged across the 10 folds and the maximum resulting accuracy score is selected as the best K features. SVM classifier is a binary classifier that aims at finding a hyperplane that maximizes the margin between the two classes. This was implemented using built in feature selection functions in Python using the Scikit-Learn library. Using this method, two volume[1] and five density[2] ICs were identified to be useful in predicting rearrest as a binary outcome (rearrest vs not). These

neural age measures identified in this feature selection step were then used in Cox proportional hazards regression predicting time to rearrest.

Cox regression takes 'time at risk' into account by using time to rearrest as the outcome variable, calculated as the number of days between release from incarceration and the rearrest date, or the follow-up date for those who were not rearrested. Arrest data was collected using a nationwide commercial search company (SSC, Inc). Those who were not rearrested are included in the analyses and considered to be 'censored' cases, meaning they potentially could still re-offend, accounting for variable lengths of follow-up. Reliability of the Cox regressions was assessed using bootstrapping with 9999 iterations. Cox regression models were computed with covariates from (Aharoni et al., 2013): PCL-R Factor 1, PCL-R Factor 2, the interaction of PCL-R Factor 1 and PCL-R Factor 2, drug and alcohol dependence, false alarm rate

---

[1] Volume components identified with feature selection: Components 14 and 24
[2] Density components identified with feature selection: Components 4, 16, 21, 24, and 26.

Table 1
Details on cohorts that were re-arrested versus not re-arrested.

	Non re-arrested group			Re-arrested group		
	N	Mean	SD	N	Mean	SD
Age at Scan	31	32.74	7.929	50	30.96	7.45
IQ	31	98.06	12.770	48	92.83	12.28
Years of education	31	10.87	2.262	50	10.28	2.52
PCL-R total score	31	22.35	6.432	47	24.32	6.94
PCL-R factor 1	31	7.45	3.075	47	7.38	3.27
PCL-R factor 2	31	13.06	3.924	47	14.64	3.58

Note. No significant differences between groups across all variables. PCL-R refers to the Hare Psychopathy Checklist-Revised.

from the Go/No Go task, ACC activity extracted from the Go/No Go task, and chronological age, as well the brain-age measures identified here. Independent samples *t*-tests were performed on these variables to assess differences between offenders who were rearrested and those who were not (see Table 1).

A total of eight Cox proportional hazards regressions were computed with rearrest as the binary DV and time-to-rearrest as the continuous DV. The models were:

> Model 1) chronological age only (replicating an analysis in (Aharoni et al., 2013) minus three participants who were excluded due to motion contaminated structural MRIs);

Model 2) chronological age and the covariates from (Aharoni et al., 2013): PCL-R Factor 1, PCL-R Factor 2, the interaction of PCL-R Factor 1 and PCL-R Factor 2, drug and alcohol dependence, false alarm rate from a Go/No Go task, Go/No Go anterior cingulate fMRI data (this model replicated that in (Aharoni et al., 2013) minus three participants who were excluded due to motion contaminated structural MRIs).

Model 3) brain volume measures of age-related components selected to be useful in predicting rearrest (i.e., 2 volume components);

Model 4) the two brain volume variables in Model 3 and covariates from (Aharoni et al., 2013): PCL-R Factor 1, PCL-R Factor 2, the interaction of PCL-R Factor 1 and PCL-R Factor 2, drug and alcohol dependence, false alarm rate from the Go/No Go task, anterior cingulate activity extracted from the Go/No Go task);

Model 5) variables in Model 4 and chronological age;

Model 6) brain-age density variables (5 density components).

Model 7) brain density components related to age and covariates from (Aharoni et al., 2013): PCL-R Factor 1, PCL-R Factor 2, the interaction of PCL-R Factor 1 and PCL-R Factor 2, drug and alcohol dependence, false alarm rate from the Go/No Go task, Go/No Go ACC activity);

Model 8) variables in Model 7 and chronological age.

In combination, these models allow for a full picture of how well brain-age measures predict rearrest, whether brain-age adds incrementally to models with chronological age, and if chronological age is necessary in models with brain-age measures. Goodness-of-fit were

Table 2
Linear stepwise regressions predicting chronological age with volume and density SBM components.

Predictors	β	t	Sig.	Predictors	β	t	Sig.
Significant volume predictors				Significant density predictors			
10	−0.186	−6.887	< 0.001	2	−0.200	−6.769	< 0.001
16	−0.308	−12.850	< 0.001	18	−0.440	−16.047	< 0.001
22	0.431	20.151	< 0.001	29	−0.291	−10.134	< 0.001
15	−0.167	−6.078	< 0.001	26	0.114	6.116	< 0.001
28	−0.147	−5.310	< 0.001	24	−0.197	−11.104	< 0.001
5	−0.160	−7.911	< 0.001	12	−0.203	−8.725	< 0.001
24	−0.293	−10.261	< 0.001	10	0.113	7.057	< 0.001
4	0.231	7.776	< 0.001	30	−0.086	−4.568	< 0.001
6	−0.153	−6.927	< 0.001	3	−0.067	−3.541	< 0.001
19	0.115	5.388	< 0.001	19	0.158	4.577	< 0.001
11	−0.067	−3.693	< 0.001	20	0.076	4.574	< 0.001
27	0.061	3.785	< 0.001	27	0.060	3.882	< 0.001
20	0.145	5.215	< 0.001	16	−0.089	−3.735	< 0.001
12	−0.099	−3.560	< 0.001	25	0.060	3.542	< 0.001
3	0.073	3.378	< 0.001	28	−0.098	−3.172	0.002
14	0.101	4.802	0.001	21	0.102	3.653	< 0.001
26	0.083	3.500	< 0.001	17	−0.070	−3.132	0.002
8	−0.130	−4.129	< 0.001	14	0.057	2.865	0.004
25	−0.070	−2.858	0.004	4	0.041	2.607	0.009
Nonsignificant volume predictors				Nonsignificant density predictors			
1	0.012	0.505	0.614	1	0.025	0.609	0.542
2	0.009	0.472	0.637	9	−155.645	−1.571	0.116
7	−0.037	−1.653	0.098	11	−0.035	−1.445	0.149
9	0.009	0.402	0.688	13	0.026	1.664	0.096
13	0.009	0.554	0.580	15	−0.015	−0.858	0.391
17	−0.026	−0.951	0.342	22	0.010	0.599	0.549
18	0.002	0.099	0.921	23	0.003	0.204	0.838
23	0.042	1.682	0.093				
29	0.024	1.384	0.167				
30	0.037	1.920	0.055				

Note. On the left side of the table is the final step of a linear stepwise regression predicting chronological age with volume SBM components. Significant components are listed in the order in which they were selected for the model. These 19 components account for 68.2% of the variance in chronological age and, taken together, are a neural measure of age. $R^2 = 0.682$, $R = 0.826$, $p < .001$. Component numbers are listed for SBM components. On the right side of the table is the final step of a linear stepwise regression predicting chronological age with density SBM components. Significant components are listed in the order in which they were selected for the model. These 19 components account for 71.0% of the variance in chronological age and, taken together, are a neural measure of age. $R^2 = 0.710$, $R = 0.843$ ($p < .001$). Components 7 and 8 are not included in above table due to having tolerance values of 0.000. Tolerance is an indication of the percent of variance in the predictor that cannot be accounted for by the other predictors; hence, very small values (e.g., 0.000) indicate a predictor is redundant. Component numbers are listed for SBM components.

calculated for each model and compared between models by calculating the Akaike Information Criterion (AIC; (Akaike, 1992)), Likelihood ratio test and Score log rank test.

3. Results

3.1. Experiment 1

Stepwise linear regressions were calculated for brain volume measures predicting chronological age. Nineteen brain volume and 19 density ICs (Figs. 1 & 2; Table 2) accounting for 68.2% and 71.0%, respectively, of the variance in chronological age. A four-dimensional NIFTI file containing these ICs is available from the corresponding author.

3.2. Experiment 2

The first two models confirmed previous analyses from (Aharoni et al., 2013): Prediction Model 1, which only tested whether chronological age negatively predicted recidivism, was significant ($p = .044$; one-tailed; Table 3). Model 2 was significant ($p = .030$) and PCL-R Factor 2 ($p = .005$), anterior cingulate activity from the Go/No Go Task in (Aharoni et al., 2013) ($p = .0005$), and chronological age ($p = .028$) were unique predictors in the expected direction (Table 3). Although chronological age was a significant predictor of re-offending in the Cox regression, post-hoc t-test indicated that age (at time of release to the community) did not significantly differ between those who re-offended and those who did not ($t(91) = 1.60$, $p = .113$). Anterior cingulate activity did differ between groups ($t(91) = 2.01$, $p = .047$) and PCL-R Factor 2 was marginally different between groups ($t(85) = 1.82$, $p = .073$).

Models 3–5, which used brain-age estimated using volume measures, were significant. Model 3 ($p = .003$), which included only brain volume components, found that Component 14 (temporal pole; $p = .039$), and 24 (interior temporal gyrus; $p = .037$) (Table 4) were significant predictors in the expected direction. Model 4 ($p = .005$) included PCL-R Factor 2 ($p = .012$), ACC activity ($p = .011$) and Component 14 (temporal pole; $p = .040$) as significant predictors in the expected directions; Component 24 was a marginally significant predictor ($p < .086$; Table 4). Model 5 ($p = .001$) included PCL-R Factor 2

($p = .014$), ACC activity ($p = .002$), chronological age ($p = .002$), Component 24 (inferior temporal gyrus; $p = .014$), and Component 14 ($p = .045$) as unique predictors (Table 4).

Using t-tests, less gray matter volume was identified for the re-arrested group, compared to the not-rearrested group, in Components 14 (temporal pole) and 24 (inferior temporal gyrus), $t(91) = 2.74$, $p = .007$, $t(91) = 3.14$, $p = .002$, respectively.

Models 6–8, which used brain-age estimated using density measures, were significant. Model 6 ($p = .004$) included Component 21 (inferior frontal/temporal pole; $p = .026$) as a predictor and Component 24 as a marginal predictor ($p < .080$; Table 5). Model 7 ($p = .003$) included PCL-R Factor 2 ($p = .006$), ACC activity ($p = .001$), and Component 21 (inferior frontal/temporal pole; $p = .010$), as unique predictors (Table 5). Model 8 ($p = .002$) included PCL-R Factor 2 ($p = .004$), ACC activity ($p = .0005$), chronological age ($p = .016$), and Component 21 (inferior frontal/temporal pole; $p = .003$) as unique predictors (Table 5).

Fig. 3 shows maps of the volume (IC 14 and 24) components and Fig. 4 shows the density (IC 21) component that were significant predictors of rearrest.

Using t-tests, less gray matter density was measured in the re-arrested group, compared to the not-rearrested group, in Component 21 (temporal pole), $t(91) = 3.53$, $p < .001$. Components 12 (cerebellum) and 26 (occipital lobe) exhibited a similar, marginally significant, relationship, ($t(91) = 1.68$, $p = .097$, $t(91) = 1.85$, $p = .067$), respectively. More gray matter density was measured in the rearrested group, compared to the not-rearrested group, in component 4 (angular gyrus), 16 (inferior parietal gyrus) and 24 (cerebellum), $t(91) = -1.99$, $p = .049$, $t(91) = -2.16$, $p = .034$, $t(91) = -2.63$, $p = .010$, respectively. Component 20 (fusiform gyrus, calcarine fissure, lingual gyrus, & and occipital lobe) exhibited a similar, marginally significant, relationship, $t(91) = -1.77$, $p = .079$.

The pattern of AIC results is consistent with the known complexity of predicting recidivism. Simple models, that included only chronological age or brain-age measures, had relatively high AIC values. Model 1 (chronological age only) was 405.62. Similarly, Model 3 (brain-age, volume) and Model 6 (brain-age, density) had high AIC's of 398.22 and 399.34, respectively. More complex models that included psychological variables and brain variables had better AIC values (Model 2 = 340.41; Model 4 = 337.19; Model 7 = 334.72; Model

Table 3
Preliminary Cox proportional hazards regressions.

Predictor	B	Boot-strapped B	SE (B)	Boot-strapped SE (B)	p-Value 2-tailed/1-tailed	Exp[B]	CI (95%) for exp[B]	Boot-strapped CI (95%) for exp[B]	Proportion of full model chi-square
Model 1 rel. age									2.92
	−0.03	−0.03	−0.02	−0.0002	**0.088/0.044**	0.97	0.93–1.01	0.93–1.00	
Model 2 PCL-R F1									0.72
	−0.06	−0.06	0.07	0.07	0.396/0.198	0.94	0.82–1.08	0.80–1.07	
PCL-R F2	**−2.60**	**−2.60**	**1.01**	**1.05**	**0.010/0.005**	**0.07**	**0.01–0.53**	**0.01–0.40**	6.67
PCL-R Int.	0.07	0.07	0.25	0.27	0.788	1.07	0.66–1.73	0.65–1.88	0.07
Drug	−0.19	−0.19	0.37	0.43	0.609	0.83	0.40–1.72	0.34–1.92	0.26
Alcohol	0.11	0.11	0.20	0.23	0.591	1.11	0.75–1.66	0.73–1.80	0.29
Go/No Go FA	−0.01	−0.01	0.01	0.01	0.571	0.99	0.97–1.02	0.97–1.02	0.32
ACC	**−0.69**	**0.69**	**0.21**	**0.23**	**0.001/0.0005**	**0.50**	**0.34–0.75**	**0.29–0.72**	11.13
Rel. age	**−0.04**	**−0.04**	**0.96**	**0.03**	**0.048/0.024**	**0.96**	**0.92–1.00**	**0.91–1.00**	3.91

Note. Results of Cox proportional hazards regression analyses examining the predictive effect chronological age (Model 1) and chronological age with covariates (Model 2) on rearrest. Model 1: Wald(1) = 2.92, $p = .088$; Likelihood Ratio(1) = 3.02, $p = .082$; $R^2 = 0.032$, Score(logrank)(1) = 2.95, $p = .086$. Model 2: Wald (8) = 17.04, $p = .030$; Likelihood Ratio(8) = 19.19, $p = .014$; $R^2 = 0.20$, Score(logrank)(8) = 17.87, $p = .022$. Variables in bold font are unique predictors within the model; one-tailed p values are provided for a priori predictors. Rel. Age is the participant's age when released from the correctional facility; PCL-R F1 and F2 refer to Factor 1 and Factor 2 scores from the Hare Psychopathy Checklist–Revised (PCL-R); PCL-R Int. refers to the PCL-R interaction term, formed by multiplying PCL-R Factor 1 by Factor 2; Drug refers to the participant's average use of the following drug classes: sedatives, cannabis, stimulants, opioids, cocaine, and hallucinogens collected from the Scheduled Clinical Interview for DSM-IV Axis I Disorders – Patient Version (SCID I/P) and the Kiddie Schedule for Affective Disorders and Schizophrenia (K-SADS); Alcohol refers to the participant's average use of alcohol collected from the SCID I/P and K-SADS; Go/No Go FA refers to the false alarm rate to NoGo stimuli; ACC refers to dorsal anterior cingulate cortex mean activation (see Aharoni et al., 2013).
Bold values significant predictors, $p < .05$.

Table 4

Cox proportional hazards regression with volume SBM components and other covariates.

Predictor	B	Boot-strapped B	SE (B)	Boot-strapped SE (B)	p-Value 2-tailed/1-tailed	Exp[B]	CI (95%) for exp [B]	Boot-strapped CI (95%) for exp[B]	Proportion of full model chi-square
Model 3									3.11
ICv 14	−0.295	−0.304	0.167	0.174	0.078/0.039	0.745	0.537–0.034	−0.626 - 0.055	
ICv 24	−0.302	−0.308	0.169	0.181	0.074/0.037	0.740	0.531–1.029	−0.626 – 0.055	3.20
Model 4		-0.047							0.40
PCL-R F1	−0.422		0.067	−0.004	0.526/0.263	0.959	0.842–1.09	−0.174–0.098	
PCL-R F2	**−2.32**	**−2.59**	**1.02**	**0.069**	**0.023/0.012**	**0.099**	**0.013–0.725**	**−4.11–0.031**	5.18
PCL-R Int.	0.074	0.075	1.017	1.06	0.752	1.08	0.681–1.70	−0.444–0.591	0.10
Drug	0.045	0.054	0.383	0.483	0.907	1.045	0.494–2.214	−0.911–0.981	0.01
Alcohol	0.002	−0.002	0.195	0.231	0.993	1.001	0.683–1.469	−0.448–0.458	0.00
Go/No Go FA	−0.005	−0.005	0.012	0.014	0.664	0.995	0.971–1.02	−0.033–0.022	0.19
ACC	**−0.436**	**−0.480**	**0.190**	**0.232**	**0.022/0.011**	**0.647**	**0.445–0.939**	**−0.845–0.063**	5.24
ICv 14	**−0.340**	**−0.377**	**0.193**	**0.221**	**0.079/0.040**	**0.712**	**0.487–1.039**	**−0.737–0.131**	3.10
ICv 24	−0.268	−0.297	0.197	0.230	0.173/0.086	0.764	0.520–1.125	−0.691–0.211	1.85
Model 5		-0.040							0.21
PCL-R F1	−0.034		0.074	0.077	0.647/0.323	0.967	0.836–1.118	−0.178–0.122	
PCL-R F2	**−2.32**	**−2.65**	**1.053**	**1.125**	**0.028/0.014**	**0.099**	**0.012–0.778**	**−4.183–0.228**	4.84
PCL-R Int.	0.249	0.271	0.253	0.286	0.325	1.283	0.781–2.107	−0.334–0.789	0.97
Drug	0.249	0.285	0.401	0.503	0.533	1.283	0.585–2.82	0.773–1.201	0.39
Alcohol	−0.009	−0.007	0.206	0.241	0.963	0.99	0.662–1.483	−0.484–0.460	0.00
Go/No Go FA	−0.009	−0.009	0.012	0.014	0.462	0.991	0.967–1.015	−0.037–0.019	0.54
ACC	**−0.576**	**−0.645**	**0.197**	**0.235**	**0.004/0.002**	**0.562**	**0.381–0.828**	**−0.967–−0.047**	8.47
Rel. age	**−0.070**	**−0.078**	**0.024**	**0.027**	**0.004/0.002**	**0.932**	**0.889–0.978**	**−0.115–−0.007**	8.35
ICv 14	**−0.336**	**−0.373**	**0.197**	**0.228**	**0.089/0.045**	**0.715**	**0.486–1.052**	**−0.746–0.147**	2.90
ICv 24	**−0.462**	**−0.523**	**0.212**	**0.249**	**0.029/0.014**	**0.629**	**0.415–0.955**	**−0.889–0.088**	4.74

Note. Results of Cox proportional hazards regression analyses examining the predictive effect neural age defined with volume SBM components (Model 3), neural age with covariates (Model 4), and neural age with covariates and chronological age (Model 5) on rearrest are presented. Model 3: Wald(2) = 11.87, p = .003, Likelihood Ratio(2) = 12.42, p = .002, R^2 = 0.125, Score(logrank)(2) = 12.02, p = .002. Model 4: Wald(9) = 23.56, p = .005; Likelihood Ratio(9) = 24.42, p = .004, R^2 = 0.252, Score(logrank)(9) = 24.96, p = .003. Model 5: Wald(10) = 29.3, p = .001; Likelihood Ratio(10) = 33.16, p = .001, R^2 = 0.326, Score(logrank)(10) = 32.97, p = .001. Variables in bold font are unique predictors within the model; one-tailed p values are provided for a priori predictors. Rel. Age is the participant's age when released from the correctional facility; PCL-R F1 and F2 refer to Factor 1 and Factor 2 scores from the Hare Psychopathy Checklist–Revised (PCL-R); PCL-R Int. refers to the PCL-R interaction term, formed by multiplying PCL-R Factor 1 by Factor 2 scores; Drug refers to the participant's average use of the following drug classes: sedatives, cannabis, stimulants, opioids, cocaine, and hallucinogens collected from the Scheduled Clinical Interview for DSM-IV Axis I Disorders–Patient Version (SCID I/P) and the Kiddie Schedule for Affective Disorders and Schizophrenia (K-SADS); Alcohol refers to the participant's average use of alcohol collected from the SCID I/P and K-SADS; Go/No Go FA refers to the false alarm rate to NoGo stimuli; ACC refers to dorsal anterior cingulate cortex mean activation (see Aharoni et al., 2013). ICv component numbers are listed for SBM volume components included in the models.

5 = 330.44; Model 8 = 332.27). In summary, Models (4, 5, 7 and 8) that included brain-age measures and psychological variables were best supported. Likelihood ratio test and Score log rank test score are presented in the tables. All reported p values indicate two and/or one tailed tests (for a priori predictors).

4. Discussion

We confirmed hypotheses that structural brain components related to age would distinguish offenders who are likely to re-offend from those who do not re-offend. Brain-age measures (Models 3: R^2 = 0.125 and 6: R^2 = 0.17) accounted for almost four times the variance in the risk equation for rearrest than did chronological age (Model 1; R^2 = 0.032). Brain-age incrementally added to risk outcomes that included other psychological and behavioral variables (Models 5 and 8) and, when neural age was included in the model with chronological age, chronological age was not necessary in predicting rearrest (Models 4 and 7). Reduced gray matter volume and density were identified as significant predictors of both neural age and rearrest. Specifically, reduced gray matter in bilateral anterior/lateral temporal lobes, amygdala, and inferior/orbital frontal cortex was helpful in predicting rearrest. This is the first prospective study to report brain-age measures predict re-offending.

The temporal pole was identified in both volume and density measures as useful in predicting age and rearrest. The temporal pole is considered to be a paralimbic region, lying between the amygdala and orbitofrontal cortex (Mesulam, 2000). Anterior and medial temporal lobe damage is classically involved in Klüver–Bucy syndrome (Klüver and Bucy, 1938), and atrophy of this region is typically implicated in

frontotemporal dementia (Hodges, 2001; Mummery et al., 2000). Both of these conditions involve symptoms that include changes in personality and socially inappropriate behavior (Thompson et al., 2003). Gorno-Tempini and colleagues studied temporal atrophy in a patient (JT) who had marked changes in behavior and personality, notably transitioning from someone who was extraverted, open, and empathic to an individual characterized by neuroticism and lacking empathy (Gorno-Tempini et al., 2004). The temporal pole is involved in theory of mind, inferring the desires, intentions, or beliefs of others (Baron-Cohen et al., 1999; Fletcher et al., 1995; Gallagher et al., 2000; Goel et al., 1995; McCabe et al., 2001; Walter et al., 2004). It is active during tasks that require subjects to think about others' thoughts and emotions (Grèzes et al., 2004) and moral decision-making (Heekeren et al., 2003; Moll et al., 2002) and while inferring the emotional states of others (Carr et al., 2003; Farrow et al., 2001; Olson et al., 2007; Völlm et al., 2006). Olson et al. (2007) suggest that the general function of the temporal pole is to couple emotional responses to highly processed sensory stimuli and storage of perception-emotion linkages for semantic memory.

Reduced gray matter volume and density in this region has been identified in psychopathic individuals (Cope et al., 2014; Ermer et al., 2012; Ermer et al., 2013; Kiehl, 2006) and has been found to be uniquely predictive of committing homicide among juvenile offenders (Cope et al., 2014). Reduced volume of the amygdala, a structure well-known to be critical for affective processing, has also been associated with psychopathic traits and longitudinal patterns of violent behavior (Pardini et al., 2014).

In the present sample, those who recidivated had lower volume in the temporal pole than did those who did not re-offend. It is reasonable

Table 5
Cox proportional hazards regressions with density SBM components and other covariates.

Predictor	B	Boot-strapped B	SE (B)	Boot-strapped SE (B)	p-Value 2-tailed/ 1-tailed	Exp[B]	CI (95%) for exp [B]	Boot-strapped CI (95%) for exp[B]	Proportion of full model chi-square
Model 6									
ICd 4	0.150	0.016	0.156	0.171	0.338/0.169	1.162	0.855–1.578	−0.362–0.395	0.92
ICd 16	0.017	0.016	0.177	0.193	0.925/0.463	1.017	0.719–1.438	−0.362–0.396	0.01
ICd 21	**−0.403**	**−0.419**	**0.207**	**0.227**	**0.052/0.026**	**0.669**	**0.445–1.003**	**−0.831–0.059**	**3.78**
ICd 24	0.215	0.229	0.153	0.175	0.160/0.080	1.239	0.919–1.673	−0.143–0.544	1.98
ICd 26	−0.082	−0.089	0.166	0.169	0.621/0.311	0.921	0.666–1.275	−0.407–0.256	0.24
Model 7									
PCL-R F1	−0.039	−0.046	0.070	0.077	0.583/0.292	0.962	0.838–1.104	−0.183–0.119	0.30
PCL-R F2	**−2.566**	**−2.986**	**1.025**	**1.163**	**0.012/0.006**	**0.077**	**0.010–0.573**	**−4.424–0.133**	**6.26**
PCL-R Int.	0.168	0.186[1]	0.251	0.288	0.503	1.183	0.724–1.933	−0.415–0.714	0.45
Drug	0.185	0.225	0.455	0.558	0.685	1.203	0.493–2.934	−0.948–1.238	0.17
Alcohol	0.058	0.059	0.216	0.273	0.790	1.059	0.694–1.020	−0.479–0.591	0.07
Go/No Go FA	−0.008	−0.008	0.014	0.015	0.578	0.992	0.965–1.02	−0.037–0.022	0.31
ACC	**−0.595**	**−0.687**	**0.195**	**0.252**	**0.002/0.001**	**0.992**	**0.376–0.808**	**−0.998 - -0.011**	**9.31**
ICd 4	0.127	0.151	0.186	0.230	0.492/0.246	1.136	0.789–1.634	−0.348–0.555	0.47
ICd 16	−0.045	−0.046	0.186	0.244	0.807/0.403	0.956	0.664–1.376	−0.524–0.434	0.06
ICd 21	**−0.630**	**−0.727**	**0.271**	**0.332**	**0.020/0.010**	**0.533**	**0.313–0.906**	**−1.184–0.117**	**5.41**
ICd 24	0.192	0.216	0.170	0.218	0.260/0.130	1.211	0.868–1.691	−0.262–0.597	1.27
ICd 26	−0.054	−0.061	0.197	0.214	0.782/0.391	0.947	0.644–1.392	−0.468–0.372	0.08
Model 8									
PCL-R F1	−0.052	−0.062	0.076	0.084	0.499/0.250	0.950	0.818–1.103	−0.207–0.124	0.46
PCL-R F2	**−2.787**	**−3.311**	**1.058**	**1.251**	**0.008/0.004**	**0.062**	**0.008–0.490**	**−4.714–0.191**	**6.94**
PCL-R Int	0.215	0.240	0.264	0.301	0.415	1.240	0.739–2.080	−0.400–0.780	0.66
Drug	0.299	0.363	0.468	0.597	0.523	1.348	0.538–3.378	−0.935–1.404	0.41
Alcohol	0.020	0.020	0.224	0.290	0.930	1.020	0.658–1.582	−0.548–0.587	0.01
Go/No Go FA	−0.012	−0.013	0.014	−0.016	0.377	0.988	0.961–1.015	−0.042–0.020	0.78
ACC	**−0.695**	**−0.820**	**0.203**	**0.265**	**0.001/0.0005**	**0.499**	**0.336–0.743**	**−1.090−−0.049**	**11.75**
Rel. age	**−0.055**	**−0.065**	**0.026**	**0.265**	**0.035/0.016**	**0.947**	**0.899–0.996**	**−1.090−−0.049**	**4.44**
ICd 4	0.153	0.174	0.182	0.031	0.400/0.200	1.166	0.815–1.666	−0.105–0.015	0.71
ICd 16	−0.133	−0.151	0.195	0.237	0.496/0.248	0.876	0.598–1.283	−0.333–0.598	0.46
ICd 21	**−0.782**	**−0.921**	**0.282**	**0.354**	**0.005/0.003**	**0.458**	**0.264–0.795**	**−0.629–0.399**	**7.71**
ICd 24	0.016	0.011	0.197	0.240	0.937/0.469	1.016	0.690–1.495	−1.338–0.052	0.01
ICd 26	−0.006	−0.011	1.923	0.217	0.974/0.487	0.994	0.680–1.450	−0.451–0.491	0.00

Note. Results of Cox proportional hazards regression analyses examining the predictive effect neural age defined with density SBM components (Model 6), neural age with covariates (Model 7), and neural age with covariates and chronological age (Model 8) on rearrest are presented. Model 6: Wald(5) = 16.97, p = .005, Likelihood Ratio(5) = 17.3, p-value = .004, R^2 = 0.17, Score(logrank)(5) = 17.3, p-value = .004. Model 7: Wald(12) = 29.96, p = .003, Likelihood Ratio(12) = 32.88, p-value = .001, R^2 = 0.324, Score(logrank)(12) = 32.05, p-value = .001. Model 8: Wald(13) = 32.2 p = .001, Likelihood Ratio(13) = 37.33, p-value = .0004, R^2 = 0.359, Score(logrank)(13) = 36.4, p-value = .001. Bold variables are unique predictors within the model; one-tailed p values are provided for a priori predictors. Rel. Age is the participant's age when released from the correctional facility; PCL-R F1 and F2 refer to Factor 1 and Factor 2 scores from the Hare Psychopathy Checklist – Revised (PCL-R); PCL-R Int. refers to the PCL-R interaction term, formed by multiplying PCL-R Factor 1 and Factor 2 scores together; Drug refers to the participant's average use of the following drug classes: sedatives, cannabis, stimulants, opioids, cocaine, and hallucinogens collected from the Scheduled Clinical Interview for DSM-IV Axis I Disorders – Patient Version (SCID I/P) and the Kiddie Schedule for Affective Disorders and Schizophrenia (K-SADS); Alcohol refers to the participant's average use of alcohol collected from the SCID I/P and K-SADS; Go/No Go FA refers to the false alarm rate to NoGo stimuli; ACC refers to dorsal anterior cingulate cortex mean activation (see Aharoni et al., 2013). ICd component numbers are listed for SBM density components included in the models.

to suspect that individuals who have lower volume of the temporal pole may be relatively limited in their ability to couple emotional responses to cues from their environment, leading to deficits in mentalizing the actions of others, or theory of mind. These inferred limitations might contribute to poor decision-making and poor outcomes (i.e., crime).

Another brain-age component identified in our models included parts of the inferior temporal gyrus (ITG). ITG is involved in higher-order levels of visual processing in the ventral stream, associated with the representation of complex object features, such as global shape and face perception (Haxby et al., 2000). The most basic roles of the ITG are processing the color and form of objects in the visual field (Kolb and Whishaw, 2013). ITG is also involved in the attribution of intention (Brunet et al., 2000) and atrophy in the right ITG is associated with theory of mind impairments in semantic dementia group (Chan et al., 2001; Irish et al., 2014). The inferior temporal cortex projects to PFC regions via the uncinate fasciculus (Ungerleider et al., 1989), a prominent white matter tract shown to be impaired in psychopathy (Motzkin et al., 2011; Wolf et al., 2015). Thus, the ITG and temporal pole play related roles in theory of mind processing and age/maturity-related deficits in these regions are reasonable markers for an increased propensity towards antisocial behavior.

The orbital frontal cortex was also identified as an age-related component predicting re-offending. The OFC plays a vital role in using positive and negative reinforcement valuation to help guide actions and to aid in decision-making (Berridge and Kringelbach, 2013; Kringelbach, 2005). Before and after decisions are made, the OFC encodes possible expected outcomes as well as their values. Following a choice, the OFC helps evaluate the value of the outcome that was chosen, relative to all other potential outcomes (Howard et al., 2015; Lopatina et al., 2015; Mcdannald et al., 2014; Rich and Wallis, 2016) including signaling regret for missed opportunities that would have resulted in better outcomes (Camille et al., 2004; Coricelli et al., 2005; Steiner and Redish, 2014). The OFC also plays a role in flexible decision-making, as it appears to be essential for reversal learning (Hamilton and Brigman, 2015; Izquierdo et al., 2013). Damage to the OFC has been associated with deficits in reversal learning, including the classic Iowa Gambling Task (Bechara et al., 1998). Individuals with reduced volume in this region may evaluate limited sets of outcomes when planning behavior. Someone with intact OFC processing may be more likely to evaluate a larger set of all potential outcomes, and be better equipped to avoid illegal activity as a result.

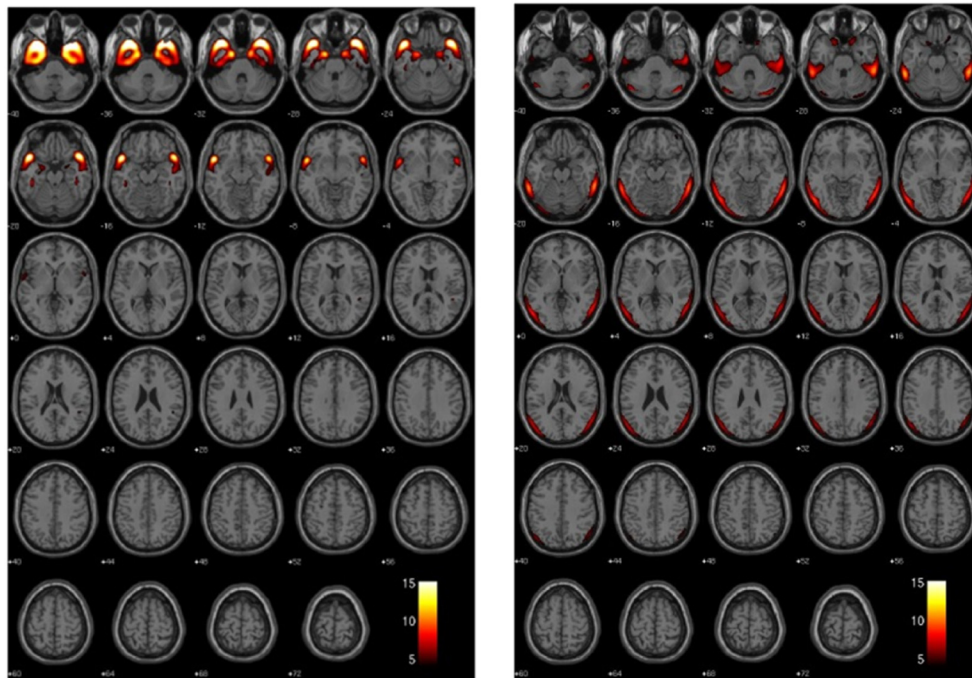Importantly, a combination of variables was most useful in

Fig. 3. Maps of the significant *volume* components (IC 14, left; IC 24, right) predicting rearrest.
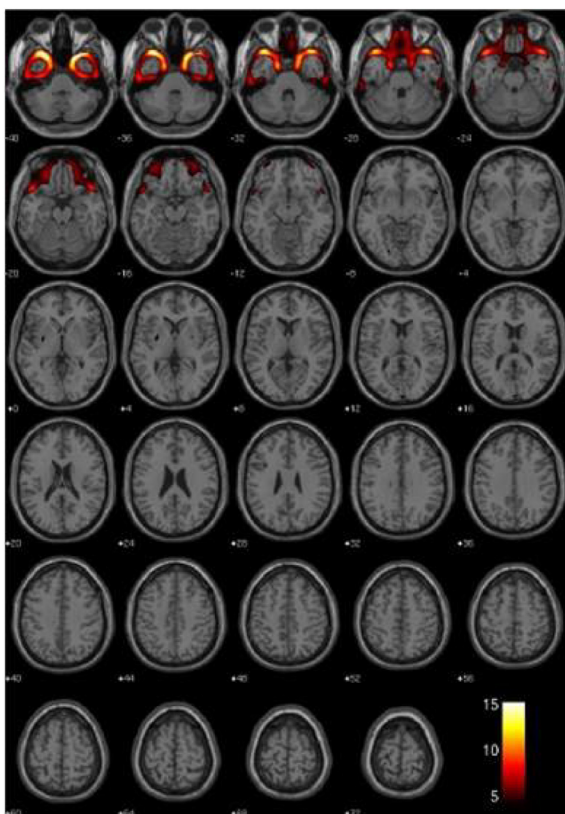

Fig. 4. Map of the significant *density* component (IC 21) predicting rearrest.

predicting rearrest in the present sample. Psychopathy scores and anterior cingulate activity elicited from a Go/No Go task had previously demonstrated utility in predicting rearrest (Aharoni et al., 2013; Steele et al., 2015). By combining structural MRI data to these measures, several additional neural regions were identified which uniquely contribute to improving prediction models. Further, structural variation in

these regions was a better indicator of future reoffending than was chronological age.

As with all studies, these findings carry a few limitations. First, our neural model of age is uni-modal and could be improved upon. For example, there are many possible brain measures that can be used as a proxy for maturity/age (Brown et al., 2012; Cao et al., 2015; Dosenbach et al., 2010; Khundrakpam, Tohka, Evans, and Group, 2015; Mwangi et al., 2013). We recommend future work integrate multi-modal brain measures (structure, function, connectivity, diffusion etc.) to produce a more comprehensive "brain maturity index". Second, from a cost-benefit perspective, measuring chronological age is far simpler and less expensive than conducting brain imaging. What is demonstrated here is that neural measures which vary as a function of age are more precise than chronological age in our prediction models. This underscores a useful theoretical distinction between one's chronological age and one's brain maturity, which progresses at different rates in individuals for a variety of reasons. As chronological age ignores these differences, it is likely to miss some important variance in helping determine future outcomes. When the stakes are relatively low, these differences may not be practically important. However, when the stakes are high vis-à-vis predicting outcomes (e.g., civil commitment of dangerous sex offenders), it may be valuable to determine these differences with the utmost precision.

This is only an initial attempt of using neural age in models predicting antisocial outcomes and does not apply to all forensic populations. For example, it is well known that different forensic groups have different risk variables. For example, inmates with traumatic brain injury have different risk needs than inmates without such injuries and individuals with mental health disorders have different risk needs than other offenders. We believe separate models will be needed for these different forensic populations.

We hypothesize that future models, including those with multi-modal neural measures (e.g. structure, function, connectivity, diffusion) and nonlinear terms, will account for more age-related variance and thus be more sensitive to specific outcomes. Moreover, future work could compute brain-psychopathy measures, brain-impulsivity measures, brain-IQ measures, to aid in the neuroprediction of rearrest. Indeed, we included only a handful of known predictors of future

rearrest. It is possible that other measures, including genetics, other demographic or psychological data, may emerge as significant predictors in future studies.

It is important to recognize that accuracy equally applies to the outcome variables as it does the predictor variables. Here we have used official arrest reports to derive our primary outcome variable (rearrest), such reports may be biased by police strategies, geography, profiling, etc. Future studies may consider using both self-report data on criminal activities as well as arrest reports to assess whether one may be more accurate than another.

4.1. Conclusions

This study demonstrated, for the first time, that structural brain imaging measures corresponding to changes in age, are useful in the prediction in future antisocial behavior. Significant predictors included areas of the medial and anterior temporal cortex (e.g. amygdala and temporal pole), and the orbitofrontal cortex. When compared directly, models using brain-age measures performed better than those using chronological age. Further, these measures incrementally improved on previously developed models that incorporate a number of other important factors, including psychopathic traits, drug and alcohol use, and functional neuroimaging data corresponding to performance on a behavioral inhibition task (Aharoni et al., 2013). As a whole, this study represents an incremental step in demonstrating the utility of brain measures for their practical predictive value; however, these findings should not be considered apart from a number of important limitations and ethical considerations. Limitations include the cost-benefit ratio for general implementation of these techniques, and the likelihood for improvement on these techniques with multimodal imaging data. Ethical considerations abound in using brain-derived information to make decisions about individuals' freedom, based on improved, but still-imperfect prediction models. Further, it demands expanded consideration of our notions of responsibility and culpability vis-à-vis behavioral variability attributable to physiological indices of maturity. We hope this work spurs on additional research for improving on these techniques and underscores the growing need for informed discourse on the ethical considerations that arise from its demonstrated utility.

Author contributions

K.A. Kiehl led the NIH/MacArthur projects that collected the data and conceived of the study approach. K.A., Kiehl, V. R. Steele, V. Rao, J.M. Maurer, K. A. Harenski, N. E. Anderson, C. Harenski, V.D. Calhoun, E. Aharoni devised and implemented the analytical approach, performed data analysis, developed interpretations, and drafted the manuscript with contributions from all the other co-authors. M. Koenigs coordinated data collection in Wisconsin prisons. All authors provided critical revisions and approved the final version for submission.

Competing financial interests

The authors do not declare any competing financial interests.

References

Aharoni, E., Vincent, G.M., Harenski, C.L., Calhoun, V.D., Sinnott-Armstrong, W., Gazzaniga, M.S., Kiehl, K.A., 2013. Neuroprediction of future rearrest. Proc. Natl. Acad. Sci. 110 (15), 6223–6228. http://dx.doi.org/10.1073/pnas.1219302110.

Akaike, H., 1992. Information theory and an extension of the maximum likelihood. In: Principle Breakthroughs in Statistics. Springer, pp. 610624.

Ashburner, J., Friston, K.J., 2000. Voxel-based morphometry–the methods. NeuroImage 11 (6), 805–821. http://dx.doi.org/10.1006/nimg.2000.0582.

Ashburner, J., Friston, K.J., 2005. Unified segmentation. NeuroImage 26 (3), 839–851. http://dx.doi.org/10.1016/j.neuroimage.2005.02.018.

Baron-Cohen, S., Ring, H.A., Wheelwright, S., Bullmore, E.T., Brammer, M.J., Simmons, A., Williams, S.C., 1999. Social intelligence in the normal and autistic brain: an fMRI study. Eur. J. Neurosci. 11 (6), 1891–1898.

Bechara, A., Damasio, H., Tranel, D., Anderson, S.W., 1998. Dissociation of working memory from decision making within the human prefrontal cortex. J. Neurosci. 18 (1), 428–437.

Berridge, K.C., Kringelbach, M.L., 2013. Neuroscience of affect: brain mechanisms of pleasure and displeasure. Curr. Opin. Neurobiol. 23 (3), 294–303.

Brown, T.T., Kuperman, J.M., Chung, Y., Erhart, M., McCabe, C., Hagler, D.J., ... Bloss, C.S., 2012. Neuroanatomical assessment of biological maturity. Curr. Biol. 22 (18), 1693–1698.

Brunet, E., Sarfati, Y., Hardy-Baylé, M.-C., Decety, J., 2000. A PET investigation of the attribution of intentions with a nonverbal task. NeuroImage 11 (2), 157–166.

Calhoun, V.D., Adali, T., Pearlson, G.D., Pekar, J.J., 2001. A method for making group inferences from functional MRI data using independent component analysis. Hum. Brain Mapp. 14 (3), 140–151. http://dx.doi.org/10.1002/hbm.1048.

Camille, N., Coricelli, G., Sallet, J., Pradat-Diehl, P., Duhamel, J.-R., Sirigu, A., 2004. The involvement of the orbitofrontal cortex in the experience of regret. Science 304 (5674), 1167–1170.

Cao, B., Mwangi, B., Hasan, K.M., Selvaraj, S., Zeni, C.P., Zunta-Soares, G.B., Soares, J.C., 2015. Development and validation of a brain maturation index using longitudinal neuroanatomical scans. NeuroImage 117, 311–318.

Caprihan, A., Abbott, C., Yamamoto, J., Pearlson, G., Perrone-Bizzozero, N., Sui, J., Calhoun, V.D., 2011. Source-based morphometry analysis of group differences in fractional anisotropy in schizophrenia. Brain Connect. 1 (2), 133–145.

Carr, L., Iacoboni, M., Dubeau, M.-C., Mazziotta, J.C., Lenzi, G.L., 2003. Neural mechanisms of empathy in humans: a relay from neural systems for imitation to limbic areas. Proc. Natl. Acad. Sci. 100 (9), 5497–5502.

Chan, D., Fox, N.C., Scahill, R.I., Crum, W.R., Whitwell, J.L., Leschziner, G., ... Rossor, M.N., 2001. Patterns of temporal lobe atrophy in semantic dementia and Alzheimer's disease. Ann. Neurol. 49 (4), 433–442.

Cole, J.H., 2017. Neuroimaging-derived brain-age: an ageing biomarker? Aging (Albany NY) 9 (8), 1861.

Cole, J.H., Leech, R., Sharp, D.J., 2015. Prediction of brain age suggests accelerated atrophy after traumatic brain injury. Ann. Neurol. 77 (4), 571–581.

Cole, J.H., Ritchie, S.J., Bastin, M.E., Hernández, M.V., Maniega, S.M., Royle, N., ... Zhang, Q., 2017. Brain age predicts mortality. Mol. Psychiatry 1–8. http://dx.doi.org/10.1038/mp.2017.62.

Cope, L., Ermer, E., Gaudet, L., Steele, V., Eckhardt, A., Arbabshirani, M., ... Kiehl, K., 2014. Abnormal brain structure in youth who commit homicide. NeuroImage: Clinical 4, 800–807.

Coricelli, G., Critchley, H.D., Joffily, M., O'Doherty, J.P., Sirigu, A., Dolan, R.J., 2005. Regret and its avoidance: a neuroimaging study of choice behavior. Nat. Neurosci. 8 (9), 1255.

Dosenbach, N.U., Nardos, B., Cohen, A.L., Fair, D.A., Power, J.D., Church, J.A., ... Lessov-Schlaggar, C.N., 2010. Prediction of individual brain maturity using fMRI. Science 329 (5997), 1358–1361.

Douglas, K.S., Webster, C.D., Hard, S.D., Eaves, D., Ogloff, J.R.P., 2002. Simon Fraser University. University of South Florida, Vancouver, BC/Tampa, FL.

Durose, M.R., Cooper, A.D., Snyder, H.N., 2014. Recidivism of Prisoners Released in 30 States in 2005: Patterns from 2005 to 2010. Bureau of Justice Statistics, Washington, DC, pp. 28.

Erhardt, E.B., Rachakonda, S., Bedrick, E.J., Allen, E.A., Adali, T., Calhoun, V.D., 2011. Comparison of multi-subject ICA methods for analysis of fMRI data. Hum. Brain Mapp. 32 (12), 2075–2095. http://dx.doi.org/10.1002/hbm.21170.

Ermer, E., Cope, L.M., Nyalakanti, P.K., Calhoun, V.D., Kiehl, K.A., 2012. Aberrant paralimbic gray matter in criminal psychopathy. J. Abnorm. Psychol. 121 (3), 649–658.

Ermer, E., Cope, L.M., Nyalakanti, P.K., Calhoun, V.D., Kiehl, K.A., 2013. Aberrant paralimbic gray matter in incarcerated male adolescents with psychopathic traits. J. Am. Acad. Child Adolesc. Psychiatry 52 (1), 94–103 (e103).

Farrow, T.F., Zheng, Y., Wilkinson, I.D., Spence, S.A., Deakin, J.W., Tarrier, N., ... Woodruff, P.W., 2001. Investigating the functional anatomy of empathy and forgiveness. Neuroreport 12 (11), 2433–2438.

First, M.B., Spitzer, R.L., Gibbon, M., Williams, J.B.W., 1997. Structured Clinical Interview for DSM-IV Axis I Disorders – Clinical Version (SCID-IV). American Psychiatric Press, Washington, D.C.

Fletcher, P.C., Happe, F., Frith, U., Baker, S.C., Dolan, R.J., Frackowiak, R.S., Frith, C.D., 1995. Other minds in the brain: a functional imaging study of "theory of mind" in story comprehension. Cognition 57 (2), 109–128.

Franke, K., Ziegler, G., Klöppel, S., Gaser, C., Initiative, A.s.D.N., 2010. Estimating the age of healthy subjects from T1-weighted MRI scans using kernel methods: exploring the influence of various parameters. NeuroImage 50 (3), 883–892.

Franke, K., Luders, E., May, A., Wilke, M., Gaser, C., 2012. Brain maturation: predicting individual BrainAGE in children and adolescents using structural MRI. NeuroImage 63 (3), 1305–1312.

Gallagher, H.L., Happé, F., Brunswick, N., Fletcher, P.C., Frith, U., Frith, C.D., 2000. Reading the mind in cartoons and stories: an fMRI study of 'theory of mind'in verbal and nonverbal tasks. Neuropsychologia 38 (1), 11–21.

Gaser, C., Franke, K., Klöppel, S., Koutsouleris, N., Sauer, H., Initiative, A.S.D.N., 2013. BrainAGE in mild cognitive impaired patients: predicting the conversion to Alzheimer's disease. PLoS One 8 (6), e67346.

Gendreau, P., Little, T., Goggin, C., 1996. A META-analysis of the predictors of adult offender recidivism: what works!*. Criminology 34 (4), 575–608. http://dx.doi.org/10.1111/j.1745-9125.1996.tb01220.x.

Goel, V., Grafman, J., Sadato, N., Hallett, M., 1995. Modeling other minds. Neuroreport 6 (13), 1741–1746.

Gorno-Tempini, M.L., Rankin, K.P., Woolley, J.D., Rosen, H.J., Phengrasamy, L., Miller, B.L., 2004. Cognitive and behavioral profile in a case of right anterior temporal lobe neurodegeneration. Cortex 40 (4), 631–644.

Grèzes, J., Frith, C., Passingham, R.E., 2004. Brain mechanisms for inferring deceit in the actions of others. J. Neurosci. 24 (24), 5500–5505.

Hamilton, D.A., Brigman, J.L., 2015. Behavioral flexibility in rats and mice: contributions of distinct frontocortical regions. Genes Brain Behav. 14 (1), 4–21.

Hare, R.D., 2003. Manual for the Hare Psychopathy Checklist - Revised, 2nd Ed. Multi-Health Systems, Toronto, Canada.

Harris, G.T., Rice, M.E., Quinsey, V.L., 1993. Violent recidivism of mentally disordered offenders the development of a statistical prediction instrument. Crim. Justice Behav. 20 (4), 315–335.

Haxby, J.V., Hoffman, E.A., Gobbini, M.I., 2000. The distributed human neural system for face perception. Trends Cogn. Sci. 4 (6), 223–233.

Heekeren, H.R., Wartenburger, I., Schmidt, H., Schwintowski, H.-P., Villringer, A., 2003. An fMRI study of simple ethical decision-making. Neuroreport 14 (9), 1215–1219.

Hodges, J.R., 2001. Frontotemporal dementia (Pick's disease): clinical features and assessment. Neurology 56 (suppl 4), S6–S10.

Howard, J.D., Gottfried, J.A., Tobler, P.N., Kahnt, T., 2015. Identity-specific coding of future rewards in the human orbitofrontal cortex. Proc. Natl. Acad. Sci. 112 (16), 5195–5200.

Irish, M., Piguet, O., Hodges, J.R., Hornberger, M., 2014. Common and unique gray matter correlates of episodic memory dysfunction in frontotemporal dementia and Alzheimer's disease. Hum. Brain Mapp. 35 (4), 1422–1435.

Izquierdo, A., Darling, C., Manos, N., Pozos, H., Kim, C., Ostrander, S., ... Rudebeck, P.H., 2013. Basolateral amygdala lesions facilitate reward choices after negative feedback in rats. J. Neurosci. 33 (9), 4105–4109.

Jain, A.K., Duin, R.P.W., Mao, J., 2000. Statistical pattern recognition: a review. IEEE Trans. Pattern Anal. Mach. Intell. 22 (1), 4–37.

Kaufman, J., Birmaher, B., Brent, D., 1997. Schedule for affective disorders and schizophrenia for school-aged children: present and lifetime version (K-SADS-PL): initial reliability and validity data. J. Am. Acad. Child Adolesc. Psychiatry 37 (7), 980–988.

Khundrakpam, B.S., Tohka, J., Evans, A.C., Group, B.D.C., 2015. Prediction of brain maturity based on cortical thickness at different spatial resolutions. NeuroImage 111, 350–359.

Kiehl, K.A., 2006. A cognitive neuroscience perspective on psychopathy: evidence for paralimbic system dysfunction. Psychiatry Res. 142, 107–128.

Klüver, H., Bucy, P.C., 1938. An analysis of certain effects of bilateral temporal lobectomy in the rhesus monkey, with special reference to "psychic blindness". Aust. J. Psychol. 5 (1), 33–54.

Kolb, B., Whishaw, I., 2013. An Introduction to Brain and Behavior, 4th ed. Worth, New York, NY.

Koutsouleris, N., Davatzikos, C., Borgwardt, S., Gaser, C., Bottlender, R., Frodl, T., ... Reiser, M., 2013. Accelerated brain aging in schizophrenia and beyond: a neuroanatomical marker of psychiatric disorders. Schizophr. Bull. 40 (5), 1140–1153.

Kringelbach, M.L., 2005. The human orbitofrontal cortex: linking reward to hedonic experience. Nat. Rev. Neurosci. 6 (9), 691.

Lopatina, N., McDannald, M.A., Styer, C.V., Sadacca, B.F., Cheer, J.F., Schoenbaum, G., 2015. Lateral orbitofrontal neurons acquire responses to upshifted, downshifted, or blocked cues during unblocking. elife 4.

McCabe, K., Houser, D., Ryan, L., Smith, V., Trouard, T., 2001. A functional imaging study of cooperation in two-person reciprocal exchange. Proc. Natl. Acad. Sci. 98 (20), 11832–11835.

Mcdannald, M.A., Jones, J.L., Takahashi, Y.K., Schoenbaum, G., 2014. Learning theory: a driving force in understanding orbitofrontal function. Neurobiol. Learn. Mem. 108, 22–27.

Mesulam, M.M., 2000. Behavioral neuroanatomy: large-scale networks, association cortex, frontal lobe syndromes, the limbic system, and hemispheric specializations. In: Mesulam, M.M. (Ed.), Principles of Behavioral and Cognitive Neurology, 2nd Edition. Oxford University Press, New York, NY.

Moll, J., de Oliveira-Souza, R., Bramati, I.E., Grafman, J., 2002. Functional networks in emotional moral and nonmoral social judgments. NeuroImage 16 (3), 696–703.

Motzkin, J.C., Newman, J.P., Kiehl, K.A., Koenigs, M., 2011. Reduced prefrontal connectivity in psychopathy. J. Neurosci. 31 (48), 17348–17357.

Mummery, C.J., Patterson, K., Price, C., Ashburner, J., Frackowiak, R., Hodges, J.R., 2000. A voxel-based morphometry study of semantic dementia: relationship between temporal lobe atrophy and semantic memory. Ann. Neurol. 47 (1), 36–45.

Mwangi, B., Hasan, K.M., Soares, J.C., 2013. Prediction of individual subject's age across the human lifespan using diffusion tensor imaging: a machine learning approach. NeuroImage 75, 58–67.

Olson, I.R., Plotzker, A., Ezzyat, Y., 2007. The enigmatic temporal pole: a review of findings on social and emotional processing. Brain 130 (7), 1718–1731.

Pardini, D.A., Raine, A., Erickson, K., Loeber, R., 2014. Lower amygdala volume in men is associated with childhood aggression, early psychopathic traits, and future violence. Biol. Psychiatry 75 (1), 73–80.

Rich, E.L., Wallis, J.D., 2016. Decoding subjective decisions from orbitofrontal cortex. Nat. Neurosci. 19 (7), 973.

Schnack, H.G., Van Haren, N.E., Nieuwenhuis, M., Hulshoff Pol, H.E., Cahn, W., Kahn, R.S., 2016. Accelerated brain aging in schizophrenia: a longitudinal pattern recognition study. Am. J. Psychiatr. 173 (6), 607–616.

Steele, V.R., Claus, E.D., Aharoni, E., Vincent, G.M., Calhoun, V.D., Kiehl, K.A., 2015. Multimodal imaging measures predict rearrest. Front. Hum. Neurosci. 9 (425), 1–13.

Steiner, A.P., Redish, A.D., 2014. Behavioral and neurophysiological correlates of regret in rat decision-making on a neuroeconomic task. Nat. Neurosci. 17 (7), 995–1002.

Thompson, S.A., Nestor, P.J., Hodges, J.R., 2003. Advances in early diagnosis and differentiation of the dementias. In: Ron, M.A., Robbins, T.W. (Eds.), Disorders of Brain and Mind. vol. 2. Cambridge University Press, Cambridge, UK, pp. 262–287.

Ungerleider, L., Gaffan, D., Pelak, V., 1989. Projections from inferior temporal cortex to prefrontal cortex via the uncinate fascicle in rhesus monkeys. Exp. Brain Res. 76 (3), 473–484.

Völlm, B.A., Taylor, A.N., Richardson, P., Corcoran, R., Stirling, J., McKie, S., ... Elliott, R., 2006. Neuronal correlates of theory of mind and empathy: a functional magnetic resonance imaging study in a nonverbal task. NeuroImage 29 (1), 90–98.

Walter, H., Adenzato, M., Ciaramidaro, A., Enrici, I., Pia, L., Bara, B.G., 2004. Understanding intentions in social interaction: the role of the anterior paracingulate cortex. J. Cogn. Neurosci. 16 (10), 1854–1863.

Wechsler, D., 1997. Wechsler Adult Intelligence Scale. Psychological Corporation, New York.

Wechsler, D., 2003. Wechsler Intelligence Scale for Children-WISC-IV. Psychological Corporation, New York.

Wolf, R.C., Pujara, M.S., Motzkin, J.C., Newman, J.P., Kiehl, K.A., Decety, J., ... Koenigs, M., 2015. Interpersonal traits of psychopathy linked to reduced integrity of the uncinate fasciculus. Hum. Brain Mapp. 36 (10), 4202–4209.

Xu, L., Groth, K.M., Pearlson, G., Schretlen, D.J., Calhoun, V.D., 2009. Source-based morphometry: the use of independent component analysis to identify gray matter differences with application to schizophrenia. Hum. Brain Mapp. 30 (3), 711–724.

Yang, M., Wong, S.C., Coid, J., 2010. The efficacy of violence prediction: a meta-analytic comparison of nine risk assessment tools. Psychol. Bull. 136 (5), 740–767.